NDT-CE 2022 - The International Symposium
on Nondestructive Testing in Civil Engineering
Zurich, Switzerland, August 16-18, 2022

Introduction of a monitoring system for Bingham fluids in additive manufacturing with concrete

Christoph STRANGFELD*, Eric SCHÖNSEE, Olubunmi Anthony JEYIFOUS, Alexander MEZHOV, Götz HÜSKEN

Bundesanstalt für Materialforschung und -prüfung (BAM), Berlin, Germany
*Corresponding author, e-mail address: christoph.strangfeld@bam.de

Abstract
Freeform additive manufacturing of concrete structures is a rising technology in civil engineering with several fascinating advantages. Nonetheless, to ensure reliability and structural integrity, standards and quality control are required in the future to bring this technology into the market. As the concrete is manufactured continuously, continuous quality control of the printing process is also required, i.e. comprehensive process monitoring. At BAM, a test rig will be installed, enabling the printing of concrete structures with a maximum size of 2 m x 1 m x 1 m (l x w x h). Here, process monitoring is the focus of the test rig. In this study, we show the results of the first pump tests, including the measurement of several parameters such as temperature and pressure along the supply system, i.e. from the concrete pump to the printer head.

Keywords: additive manufacturing of concrete, process monitoring, non-destructive testing, Bingham fluid

1 Introduction

“3D printing: The new industrial revolution”, postulated by Berman in 2012 [1]. Indeed, this statement holds for several industrial sectors and materials [2]. Meanwhile, customer-ready 3D printers utilising primarily polylactic acid (PLA), acrylonitrile butadiene styrene (ABS), etc. are commercially available. Regarding the construction sector, 3D printing of concrete structures is still a small niche market, although with high potential. Avoiding formwork during construction enables new and futuristic concepts and designs for architects and civil engineers [3][4]. Thus, direct ink writing for cement-based materials, commonly referred to as 3D concrete printing (3DCP), is an upcoming technology that has gained more and more attraction during the past years [5][6]. Nowadays, entire single-floor houses [7], school buildings[8], loft conversions, and multilevel houses [9] have been constructed. Besides the opportunities of freeform constructions, 3DCP is promoted for its potential economic benefits. In the future, automated printers might reduce the required staff on the construction site and accelerate the construction speed. Formwork causes around 35 % of the total cost of concrete structures and can grow up to 60 % for complex geometries [6]. Furthermore, 3DCP is considered a jump technology to increase labour productivity in the construction industry, which has continuously declined for decades[10]. Globally, the cement industry causes about 8 % of CO_2 emissions [11] and is estimated to grow by 12 – 23 % until 2050 [12]. Based on 3DCP, replacing massive constructions with lightweight constructions might save up to 30 % of concrete. Unfortunately, the saving effect is reduced partially by the material design itself. In 3DCP, the aggregate size is highly reduced to ensure pumpability. Concrete printing is a misleading term because the material used in 3DCP compares to screed or mortar and thus involves a higher amount of cement within the mixture. Nevertheless, the overall effect regarding CO_2 emissions is still estimated to be positive as less material is used [13]. Although this new technology inspires dreaming of a fundamentally new way of building, the current challenges in 3DCP are enormous.

In conventional construction, large amounts of concrete are mixed and placed in the formwork batchwise. Then, the concrete remains for days or even weeks inside the formwork. During this period, the hydration progresses with significant variations in flowability, stiffness, microstructure and compressive strength, etc. [14]. In most cases, the quality assurance of the concrete happens ex-post after 28 days based on retained samples collected during concreting. This is a well-established approach which is standardised [15]. On the other hand, in 3DCP, the concrete is mixed and manufactured continuously. The nozzle cross-section has only a few centimetres; hence, only small amounts of concrete are extruded at once. Furthermore, the entire material is transported via a closed tube system, with a pump pressure of up to 3 MPa. The tube diameter has only a few centimetres as well. Thus, the used concrete or mortar must fulfil several additional properties compared to conventional concrete. The additional requirements are pumpability, extrudability, open time, and green strength [16]. These four requirements behave like antagonistic to each other [17]. Therefore, every cement-based mortar mixture used for 3DCP is always a compromise and must be carefully adapted to the printing process, the environmental conditions, and the usage of the final structure. Several studies exist to influence the rheology during the printing process [18][19][20][21]. Nevertheless, several challenges remain in developing "printable concrete" for additive manufacturing [22].
Even if a perfect mixture for 3DCP is found, the printing process is still continuously. Thus, it must be ensured that the mixture properties remain within the given limits during the entire process [23]. Changes in ambient conditions or variation in the mixture composition might lead to significant quality deterioration and, eventually, compromise structural integrity. The underlying reasons can be trivial, e.g., a temporarily reduced supply of mixing water or a local blockage in the tube system during printing. Without permanent process monitoring, the quality is almost impossible to evaluate because weak spots might occur only locally. Although process monitoring is crucial to establishing this new construction technology in the market and society, neither commercial measurement techniques nor established standards exist so far [24][25]. Without international standards and methods for quality assessment, 3DCP will remain in niches without any significant economic impact on the construction industry. Standards, permanent process monitoring, and in situ quality assessment are the basis for bringing 3DCP into the market [26].
BAM is currently developing a test setup for additive manufacturing (AM) for freeform construction, where a monitoring system is installed to observe different parameters of the fresh concrete and the printed structure during the printing process. This comprehensive monitoring allows to control different parameters, either for the fresh concrete (like water content and chemical admixtures) or the pump speed and the printing path. In addition, there is a variety of equipment for conventional testing of concrete available at BAM to compare the measurements of the monitoring system with established parameters nowadays used for concrete quality control. Once the 3D concrete printer is established, the system will also be used to optimise the printing mortar.

2 Design of the test rig for additive manufacturing of concrete

3DCP enables manufacturing of arbitrarily shaped concrete structures, including all sorts of convex or concave surfaces. The designated test rig at BAM will be a gantry system with an effective printing volume of 2 m x 1 m x 1 m (length x width x height). The focus of the test rig is the evaluation of the used 3DCP mortar based on detailed process monitoring and non-destructive testing. Only "simple" structures like walls or columns will be manufactured.

Nevertheless, these simpler structures can be considered as finite sub-elements of larger structures in which the mortar can be analysed and optimised for the real object. The mortar properties will be measured in situ and instantaneously by non-destructive measuring techniques to enable a closed-loop mortar characterisation during the printing process. These non-destructive methods will be evaluated at BAM based on traditional laboratory tests. This validated test rig helps to establish international standards for 3DCP and to certify new mortars. For this purpose, standard sub-elements are considered as the optimal approach.

2.1 3DCP test rig at BAM

A CAD rendering of the designated test rig is shown in Figure 1. The printer, a gantry system, consists of three orthogonal axes. Replaceable wooden formwork panels are used as print bed. An indoor crane can move and displace the printed structure. The maximum speed of the traverses is 5 m/s, and its acceleration is at a theoretical maximum of 50 m/s^2 for a load of 50 kg. The controlling and the data acquisition is run by an industrial SPS controller.

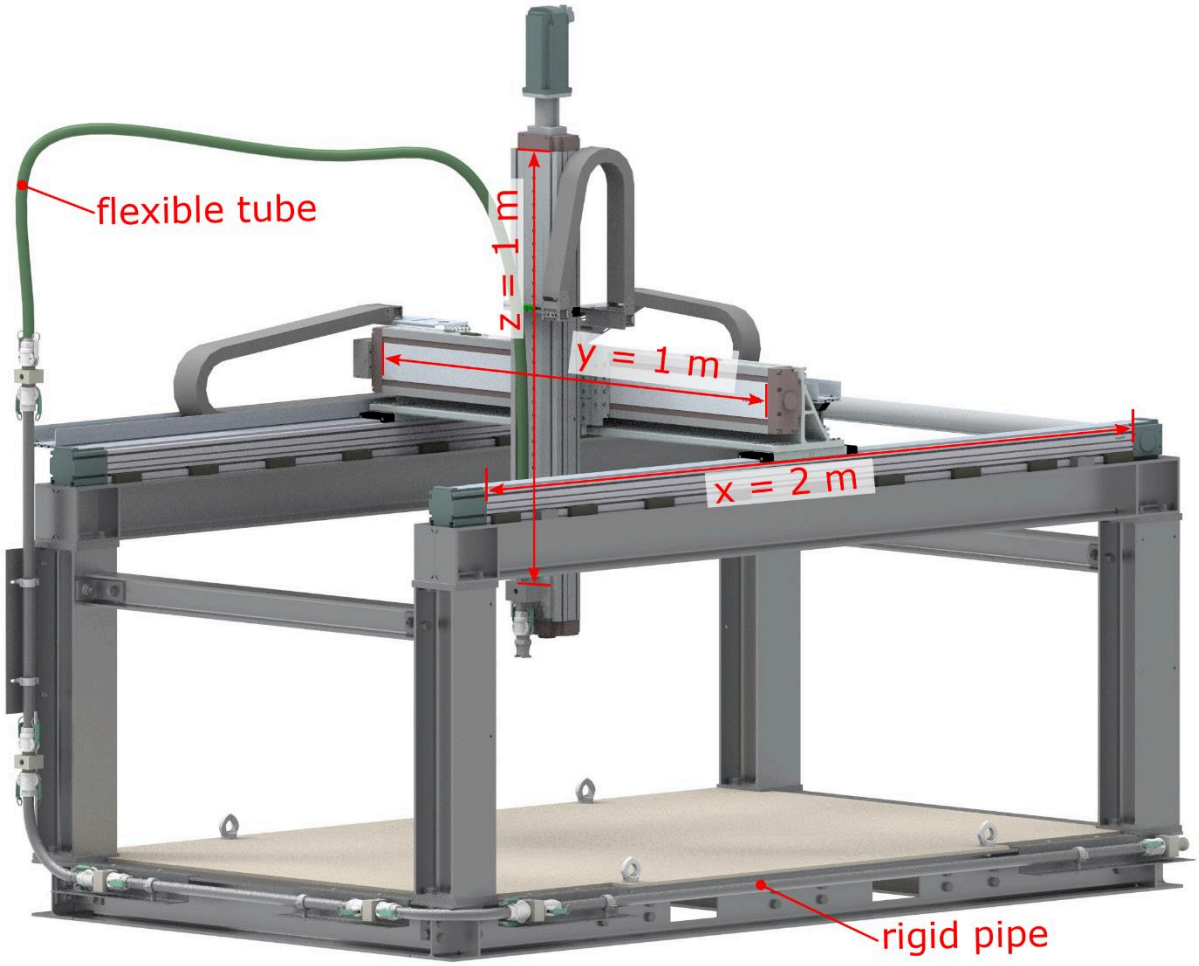

Figure 1: CAD drawing of the test rig for additive manufacturing at BAM having an effective printing volume of 2 m x 1 m x 1 m (length x width x height)

A mixing pump (m-tec duo-mix connect) is used in the test rig to mix and pump the 3D-printing mortar. The concrete pump consists of a mixing unit and a worm pump that can be controlled

separately. Furthermore, the mixing pump allows the integration into higher-level automation processes by different interfaces.
The tube system for pumping the mortar consists mainly of two sections. The first part is a highly flexible standard mortar hose, ranging from the printer scaffold to the printer head. The second part is a fixed, rigid steel pipe with a total length of about 4.5 m, which is used for mortar characterisation. It is fixed at the printer scaffold to avoid movement during the printing. Based on the fixed pipe system, pressure measurements are comparable during different test runs. Hence, changes in the pressure drop can be correlated directly to the fluid properties of the used mortar.

2.2 Measurement devices for mortar characterisation

The four main properties of 3DCP mortars are pumpability, extrudability, open time, and green strength, and it is difficult to fulfil all requirements - it is always a compromise. For example, green strength and extrudability can only be achieved in a specific range of material yield stress of around 1.5 kPa – 2.5 kPa [18][23]. Thus, these properties need to be measured and quantified to optimise the mixture for the desired purpose. Some data are measured by the concrete pump, such as rotational speed, water supply, pressure, and temperature of the pump. In addition, along the rigid pipe, two temperature sensors, and four pressure sensors are installed. The latter enables the calculation of the pressure drops, which highly correlates to the properties of the mortar and its extrudability. In a future step, a new printer head will be designed, allowing the continuous injection of additives. Thus, the measured parameters of the pipe system serve as input parameters for an optimised mixing within the printer head.

3 Experimental setup

In the current study, the focus is the mortar supply system including the installed sensors to evaluate the continuous quantification of material properties.

3.1 Setup of the pump test and its process monitoring

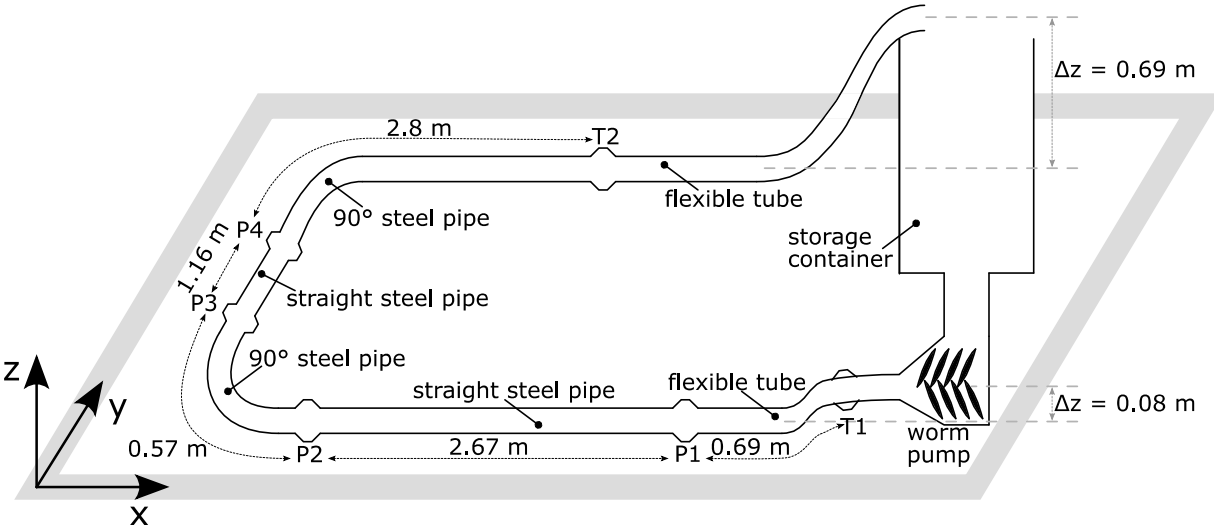

Figure 2: Schematic sketch of the setup for the pump test

In this setup, the worm pump pushes the mixture through flexible tubes connected with the rigid pipe with an inner diameter of 25 mm. In order to allow proper cleaning, especially at the

contact surface of the pressure and temperature sensors, the sensors are installed via modules for mortar couplings. The end of the rigid pipe is connected to the storage container of the pump with another 25 mm flexible tube. This setting closes the circuit and keeps material consumption low and ensures constant mixture properties. A sketch of the test setup can be seen in Figure 2.
The distance between the sensors composes of the pipe length itself, as well as the mortar couplings and sensor modules in between the pipes. This results in 0.69 m between the first temperature sensor, T1 and the first pressure sensor, P1. Going further, at the first straight pipe, there are 2.67 m between the sensors P1 and P2. The 90° bend is constructed with a radius of 0.2 m with a straight end of 0.13 m. Overall, the 90° bend has a total length of 0.57 m between P2 and P3. Along the second straight pipe, between P3 and P4, the distance is 1.16 m. After a second 90° bend, a mortar coupling to a flexible tube was installed, which leads to the second temperature sensor. From P4 to T2, it is a total length of 2.8 m. Hence, the overall distance between T1 and T2 is 7.89 m.
The difference in height from the worm pump to the sensors is 0.08 m, and the input to the storage container is at a height of 0.69 m.

3.2 Recording of the printing parameters

WIKA S-20 pressure sensors are used, which are designed for absolute pressures of up to 4 MPa and transmit an output signal from 4 mA to 20 mA. A diaphragm seal suitable for abrasive media is installed between the pipe system and the sensor to avoid damaging the pressure sensor membrane.
The temperature is acquired with multiple four-wired resistance temperature detectors (RTDs) type Pt 100 in different positions. Those are placed in the pipe and immersed in concrete. The signal of the RTDs is given to a temperature transmitter module.
A data acquisition system from National Instruments (NI USB-6210) was connected to the computer with a LabVIEW software running to record the data. Therefore, it was necessary to wire the sensors to a repeater power supply, which converts the signals from 4 mA to 20 mA into 2 V to 10 V. The temperature transmitter output is a signal from 0 V to 10 V for a range of 0 °C to 50 °C. While pumping, signals were recorded with a sampling rate of 1 kHz.
For the data evaluation, only every fiftieth value was used. Then, a running average including 75 samples was used to smooth the data and reduce the influence of noise and periodic pressure fluctuations of around 2 Hz to 10 Hz due to the worm pump. Thus, each data point represents a time period of 3.75 seconds.

3.3 Mortar properties

A non-reactive pumpable mortar was designed according to the design principles given in [27] to be used as inert model system for the pumping process. Therefore, limestone powder was used to prevent possible effects on the measurements caused by the beginning cement hydration. The mix design and relevant, fresh mortar properties are given in Table 1. The fresh mortar was tested for consistency [28], setting behaviour [29], and its rheological properties. A Bingham regression was used to determine yield stress and plastic viscosity by considering shear rates larger than 12 s^{-1}. The setting behaviour was determined using an automatic Vicat device (ToniSET supplied by Toni Technik Baustoffprüfsysteme GmbH). The rheological properties were determined using a Schleibinger Viskomat NT with a basket cell according to the measuring procedure suggested in [30]. The fresh mortar showed neither significant changes

in its consistency nor in the rheological properties, as demonstrated by the results depicted in Table 1 and Figure 3 for the estimated time interval (90 min) of the pumping test. Furthermore, the mortar showed no setting for about 18 hours after mixing (see Figure 4).

Table 1: Mix design and properties of the non-reactive mortar

Material	**Amount (kg/m³)**
Limestone powder	650.0
Micro silica	45.5
Sand 0.1-0.5	797.8
Sand 0.5-1.0	375.5
Water	308.8
Superplasticizer	3.770
Starch-based stabiliser	0.650

Property		**Value**
Flow value (mm) after [DIN EN 1015-3]	15 min	209
	30 min	211
	90 min	205
Yield stress (Pa)		207 ± 30
Plastic viscosity (Pa·s)		1.9 ± 0.2

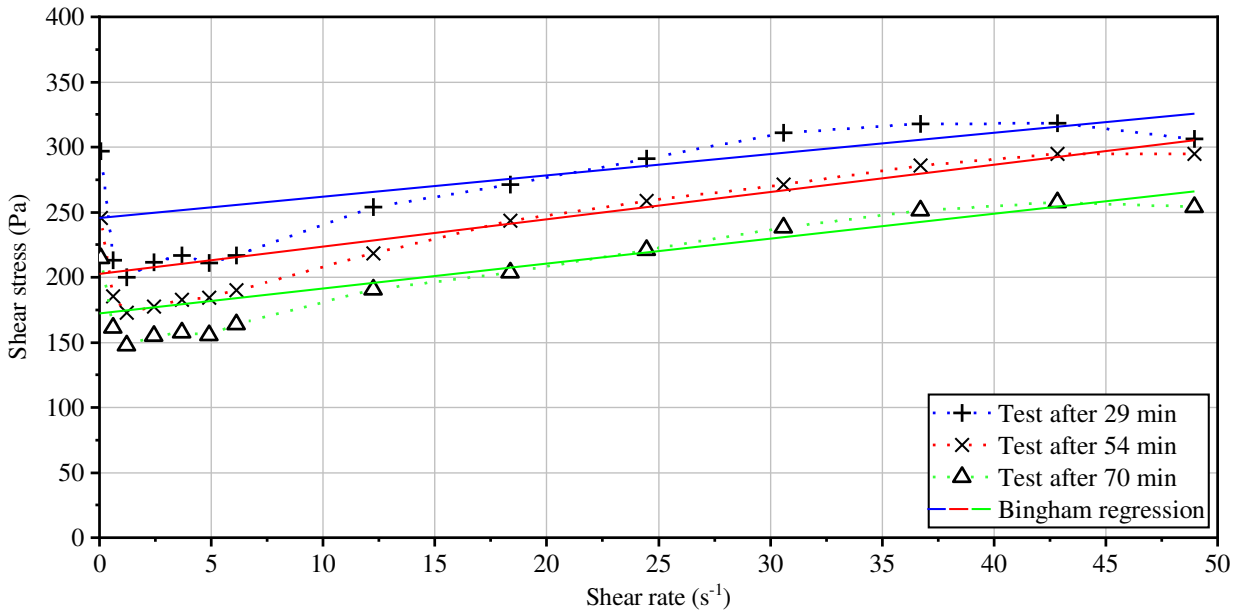

Figure 3: Flow curves expressed as shear rate versus shear stress determined at different time steps after mixing

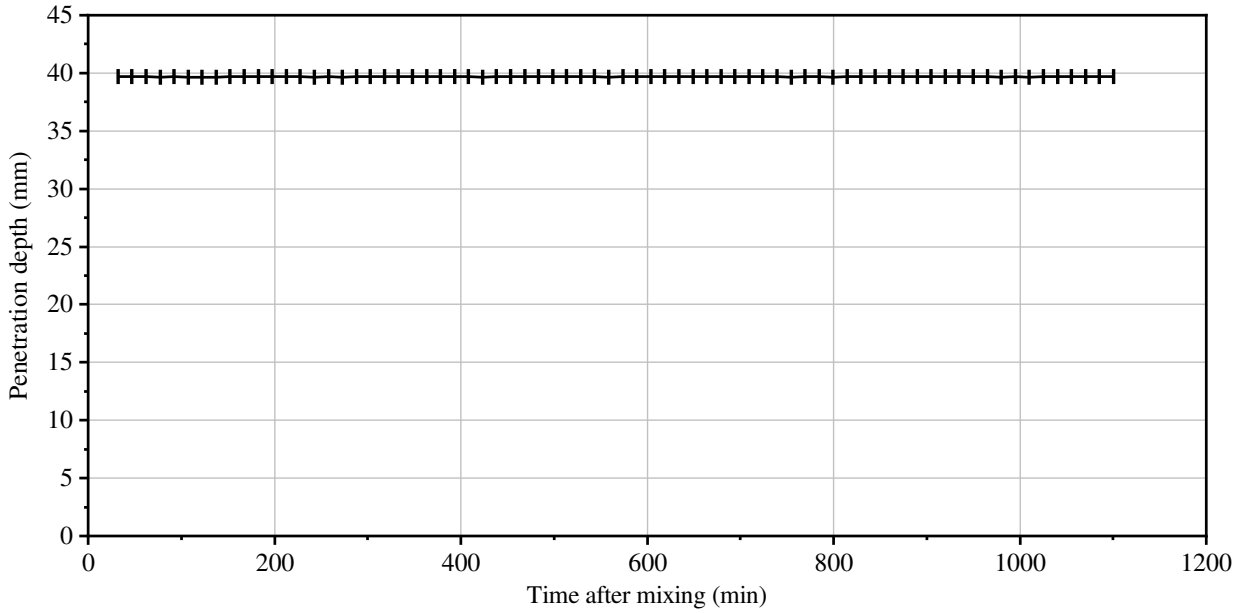

Figure 4: Penetration depth of the Vicat needle into the mortar as function of time. The height of the mould was 40 mm

4 Results and discussion

Figure 5 shows the measured pressure and temperature during the first pumping test of the limestone powder mortar. The mortar was mixed in a compulsory mixer. Thus, the mixer unit of the concrete pump was not used. The pre-mixed material was added directly into the reservoir of the worm pump. The overall data recording took around 20 minutes. After setting up the data acquisition system and filling the reservoir, the first pumping started. This is symbolised by the red highlighted area in Figure 5. At this point, the supply system was open, the mortar was pumped into a tub, and the pressure sensors recorded the increasing pressure consecutively according to their position in the system. The time delay is due to the different distances between the sensors and the worm pump. The short interruption within the red highlighted zone is due to a second reservoir filling. First, a low viscous paste of limestone powder was transported via the tube system into the tub. After a while, a homogeneously mixed mortar was continuously carried out. At this point, the pumping was stopped to connect the open end directly to the reservoir of the worm pump. During the initial pumping, the temperature increased slightly.

After connecting the tube to the reservoir, the pumping was started again in a closed supply loop, and the material was pumped continuously into the storage container of the worm pump, where a pressure equalisation took place. Thus, the counter pressure was always one standard atmosphere, although the supply runs in a closed loop. First, the volume flow rate was alternated several times by varying the rotational speed of the worm pump. This period is highlighted in green in Figure 5. The pressure follows the different flow rates, and there is no time delay between the sensor response. On the other hand, the temperature increases continuously due to friction effects in the worm pump. Due to the closed loop pumping, the generated heat is not released with the material extraction anymore. The material passes and re-enters the worm pump and thus is heated up all the time. It can be observed, that the sensor T2 consistently

shows a lower temperature, compared to T1, once the tube is filled. It is assumed that the steel pipe works as a cooling element during the process. The offset during the first 30 seconds is led back to the introduction of the low viscous limestone powder, which cooled down T1 a bit but did not reach both sensors.
Within the blue highlighted area, the concrete pump remained at a constant volume flow rate or rotational speed, respectively. In this state, ordinary tap water was introduced into the reservoir of the worm pump. The light blue area depicts the first water addition and the dark blue the second addition. This coincides with a temporary decrease in the temperature. Before water addition, the material showed a temperature of about 34 °C. Thus, the tap water can be considered to generate a slight cooling effect. However, as the pumping continues, the temperature increases again. The two water additions lead to a significant reduction of the pressure in the tube system. Due to the increase in the water to powder ratio, the mortar became more fluent, which reduced the pressure drop. After a while of mixing, a new steady state is reached, e.g. at around 0.3 MPa for pressure sensor P1, indicating that the added water is mixed and distributed homogenously in the system. For pressure sensors P2 to P4, a kind of oscillation is visible within the first two minutes after the first water addition. One period is about 45 seconds long. This correlates with one full transit of the tube system. However, further experiments are required to verify this. After switching off the pump system at about 1200 seconds, a decrease in temperature is visible because no energy is put into the system anymore. Also, the heat is released to the ambient, mainly via the metal pipes.

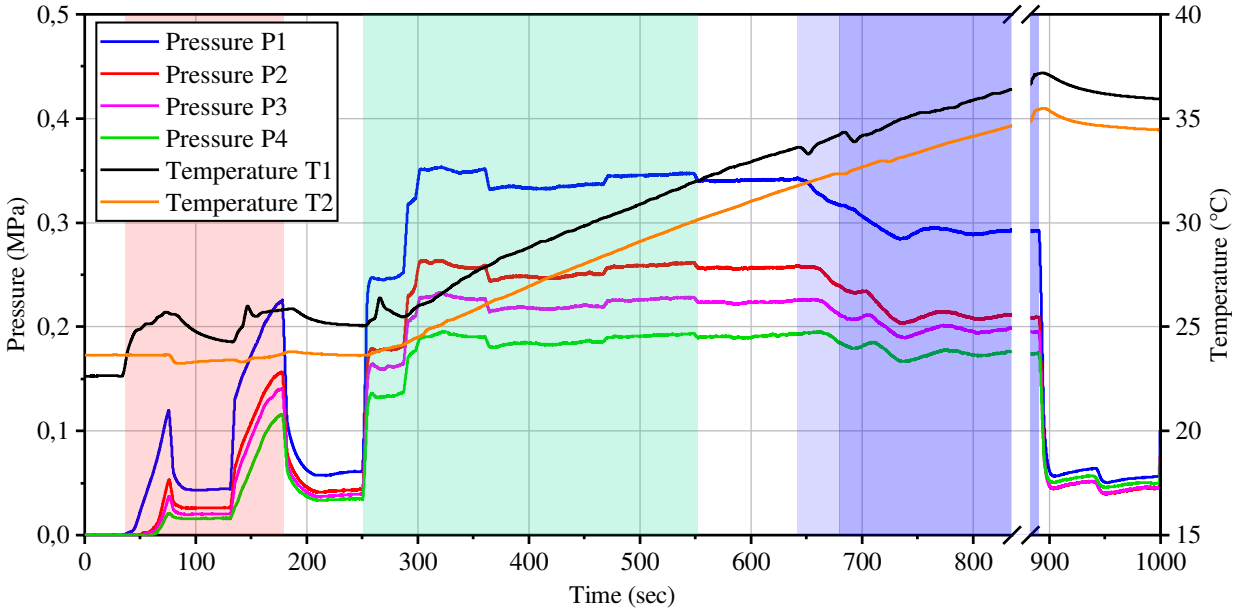

Figure 5: Evolution of the pressure and temperature during the pump tests

The measured total pressure is influenced by several parameters such as the supply pressure, the hydrostatic pressure, the material density, and the flow rate. In Figure 5, the pressure is at different, relatively constant levels in the range from 250 seconds to 600 seconds. Those levels correlate with a change in pump speed, which was changed from a speed level of 65 to 70 in different periods. After the data acquisition, the material was pumped into a container for a certain time interval. Then, the extracted material was weighed. The time interval and the mass, both give us a mean mass flow of 0.26 kg per second for a speed level of 65. It is also of interest

that the temperature reduction can be observed in both sensors, T1 and, with a delay of approximately 32 seconds in T2. Based on the distance between T1 and T2, a velocity of 0.25 m/s can be estimated. The inner diameter of the pipe is 25 mm. Although the measurement of the pressure drop might indicate a Bingham fluid, the exact velocity profile remains unknown. However, as a first highly simplified approach, one might assume a constant flow velocity over the entire cross-section. Based on this assumption, the calculated volume flow is 0.68 l/min. Even though this is a rough approximation, it results in a density of the material of around 2300 kg/m³. As the boundary layer is ignored in this approach, this density is the upper limit, and the real density would be below 2300 kg/m³. Furthermore, during mixing, air bubbles might be introduced into the mortar, which also affects the density. However, for comparison, based on the mortar formulation, the predicted density is about 2140 kg/m³. Thus, this rough and very simplified approach already gives reasonable and consistent values.

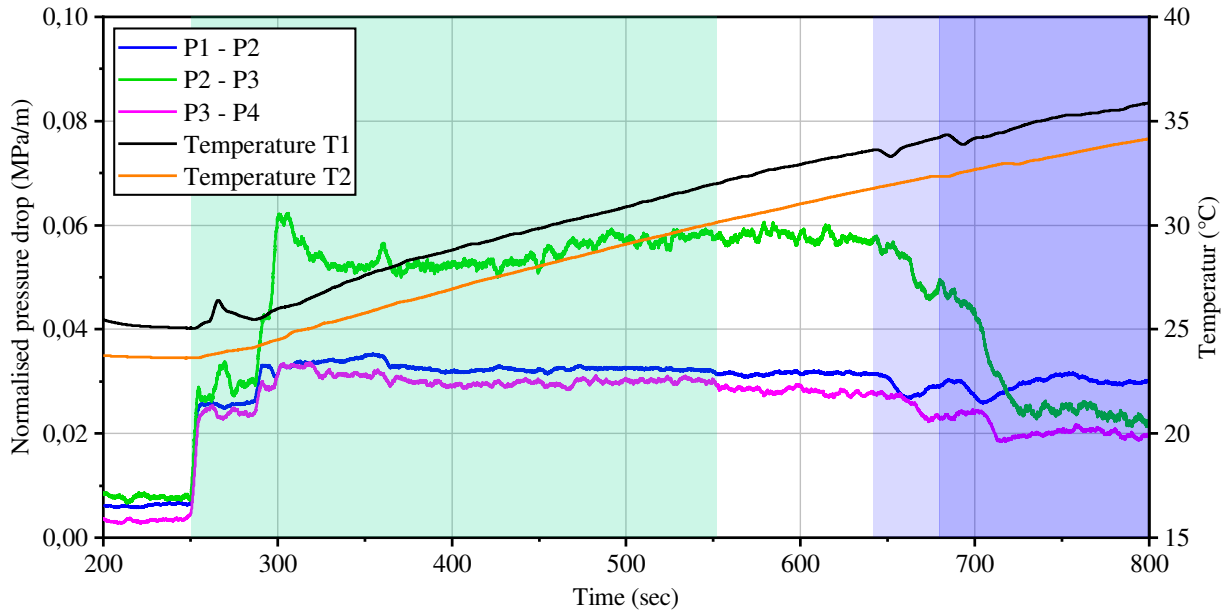

Figure 6: Evolution of the pressure drop due varying flow rates and water addition

To account more for the material properties, the pressure drop is calculated in Figure 6. Please note that for better visibility, the x-axis is restricted in Figure 6. The three pressure differences are normalised by the distance between two adjacent measurement positions. Whereas sensors P1 and P2, as well as P3 and P4, are connected to two straight pipes, sensors P2 and P3 have a curved pipe of 90° at a radius of 0.2 m in between. Although the distance between P2 and P3 is the lowest with 0.57 m, the pressure drop is the highest. It seems that the curvature significantly affects the pressure drop, probably due to Coriolis forces. Assuming a Bingham fluid which includes a plug flow, it is presumable that the higher pressure drop in a bend is caused by the break of the plug [31]. Furthermore, a variation of the volumetric flowrate also shows the most significant effects between P2 and P3. The normalised pressure drop for the two straight pipes correlates to each other during the volume flow rate variations. Between about 550 and 650 seconds, one might observe a slight decrease of all three pressure drops. This could be the influence of the increased temperature, which might lead to a viscosity reduction. By adding water, the trend for the pressure drop changes totally. In comparison, P1-P2 remains almost constant, and the other two decrease. Here, P2-P3 drops by about 0.03 MPa, and P3-P4

decreases only by about 0.01 MPa. On the one hand, the installed measurement setup shows high sensitivity to even minor variations of the material properties. On the other hand, further experiments including reference methods for data validation are required to separate all influencing factors.

5 Conclusion

To bring additive manufacturing of concrete more to the market and construction branch, a permanent quality control of the entire printing process based on international standards is required. As an initial step, a test rig to quantify mortar properties during the printing process is installed at BAM. The first pumping test, including pressure and temperature sensors, was performed with a non-reactive mortar. All sensors showed high sensitivity to variations in the water to powder ratio, volume flow rate, and mortar temperature. The normalised pressure drop varies significantly between the different sections of the pipe system. The highest normalised pressure drop is recognised in the 90° bent section. This behaviour is assumed to be caused by the break of the plug flow of the Bingham fluid. Further measurements, including different types of mortar, will be performed.

Acknowledgements
The authors gratefully acknowledge the financial support of the present work through the Federal Ministry for Economic Affairs and Climate Action within the funding program TTP Leichtbau, grant number 03LB5005.

References

[1] B Berman, '3-D printing: The new industrial revolution', Business Horizons, Vol 55, No 2, pp 155–162, 2012.
[2] Vinayagam, Mohanavel & Ali, Ashraff & Ranganathan, K & Jeffrey, J & Ravikumar, M & Rajkumar, s. (2021). The roles and applications of additive manufacturing in the aerospace and automobile sector. Materials Today: Proceedings. 47.
[3] T Wangler, E Lloret, L Reiter, N Hack, F Gramazio, M Kohler, M Bernhard, B Dillenburger, J Buchli, N Roussel and R Flatt, 'Digital concrete: opportunities and challenges', RILEM Technical Letter 1, pp 67–75, 2016.
[4] S Lim, R A Buswell, T T Le, S A Austin, A G F Gibb and T Thorpe, 'Developments in construction-scale additive manufacturing processes', Automation in Construction, Vol 21, pp 262–268, 2012.
[5] G De Schutter, K Lesage, V Mechtcherine, V N Nerella, G Habert and I Agusti-Juan, 'Vision of 3D printing with concrete – Technical, economic and environmental potentials', Cement and Concrete Research, Vol 112, pp 25–36, 2018.
[6] E Lloret, A R Shahab, M Linus, R J Flatt, F Gramazio, M Kohler and S Langenberg, 'Complex concrete structures: Merging existing casting techniques with digital fabrication', Computer-Aided Design, Vol 60, pp 40–49, 2015.
[7] 3dprintedhouse. (2021, April 30)“First resident of 3D-printed concrete house receives key” https://www.3dprintedhouse.nl/en/news/5257/first-resident-of-3d-printed-concrete-house-receives-key/ (accessed 24.06., 2022)
[8] H. Everett. (2021, July 1) “World’s first 3D printed school built with cobod construction printer welcomes students” https://3dprintingindustry.com/news/worlds-

first-3d-printed-school-built-with-cobod-construction-printer-welcomes-students-192167/ (accessed 24.06., 2022)
[9] WDR. (2021, July 21) "Ein Haus in Schichtarbeit." https://www.tagesschau.de/wirtschaft/haus-aus-dem-drucker-101.html (accessed 24.06., 2022).
[10] H H Neve, S Wandahl, S Lindhard, J Teizer, J Lerche, 'Determining the relationship between direct work and construction labor productivity in North America: four decades of insights', Journal of Construction Engineering and Management, Vol 146, No 9, 2020.
[11] World Wildlife Fund, 'Klimaschutz in der Beton-und Zementindustrie-Hintergrund und Handlungsoptionen', World Wildlife Fund Deutschland, Berlin, 2019.
[12] United Nations and International Energy Agency, 'Global status report for buildings and construction (2019) ', Vol 15, 2020.
[13] H. Abdalla, K. P. Fattah, M. Abdallah, and A. K. Tamimi, “Environmental Footprint and Economics of a Full-Scale 3D-Printed House,” Sustainability, vol. 13, no. 21, p. 11978, Oct. 2021
[14] D Wang, C Shi, N Farzadnia, Z Shi, H Jia and Z Ou, 'A review on use of limestone powder in cement-based materials: Mechanism, hydration and microstructures', Construction and Building Materials, Vol 181, pp 659–672, 2018.
[15] DIN EN 206-1/DIN 1045-2, Beton - Festlegung, Eigenschaften, Herstellung und Konformität Deutsche Norm, 2017
[16] T T Le, S A Austin, S Lim, R A Buswell, A G F Gibb and T Thorpe, 'Mix design and fresh properties for high-performance printing concrete', Material and Structure, Vol 45, No 8, pp 1221–1232, 2012.
[17] A Kazemian, X Yuan, E Cochran and B Khoshnevis, 'Cementitious materials for construction-scale 3D printing: Laboratory testing of fresh printing mixture', Construction and Building Materials, Vol 145, pp 639–647, 2017.
[18] A. U. Rehman and J-H. Kim, '3D concrete printing: A systematic review of rheology, mix designs, mechanical, microstructural, and durability characteristics', Materials, Vol 14, No 14, 2021.
[19] T T Le, S A Austin, S Lim, R A Buswell, R Law, A G F Gibb and T Thorpe, 'Hardened properties of high-performance printing concrete', Cement and Concrete Research, Vol 42, No 3, pp 558–566, 2012.
[20] M J Lynch, 'Investigation of Chemical Admixture Interactions in the Development of Printable Concrete’, The UNSW Canberra at ADFA Journal of Undergraduate Engineering Research, Vol 4, No 1, pp 1–20, 2011.
[21] A Perrot, D Rangeard and A Pierre, 'Structural built-up of cement-based materials used for 3D-printing extrusion techniques’, Materials and Structures, 2015.
[22] Y. Chen, S. He, Y. Gan, O Copuroglu, F. Veer and E. Schlangen, 'A review of printing strategies, sustainable cementitious materials and characterization methods in the context of extrusion-based 3D concrete printing', Journal of Building Engineering, Vol 45, 2022.
[23] A V Rahul, M Santhanam, H Meena and Z Ghani, '3D printable concrete: Mixture design and test methods', Cement and Concrete Composite, Vol 97, pp 13–23, 2019.
[24] V N Nerella, and V Mechtcherine, 'Studying printability of fresh concrete for formwork-free concrete onsite 3D printing technology’, 3D Concrete Printing Technology, 2019.

[25] S H Ghaffar, J Corker, and M Fan, 'Additive manufacturing technology and its implementation in construction as an eco-innovative solution', Automation in Construction, Vol 93, pp 1–11, 2018.
[26] P Wu, J Wang, X Wang, 'A critical review of the use of 3-D printing in the construction industry', Automation in Construction, Vol 68, pp 21–31, 2016.
[27] W Schmidt, B Mota, A Ramirez, 'Einfluss der Gesteinskörnung auf die Rheologie von Beton', BWI – BetonWerk International, Vol 21, pp 42-51, 2018
[28] DIN EN 1015-3, 'Methods of test for mortar for masonry - Part 3: Determination of consistence of fresh mortar (by flow table)', Deutsches Institut für Normung e.V., 2007
[29] DIN EN 480-2, 'Admixtures for concrete, mortar and grout - Test methods - Part 2: Determination of setting time', Deutsches Institut für Normung e.V., 2006
[30] M Haist, J Link, D. Nicia, et al., 'Interlaboratory study on rheological properties of cement pastes and reference substances: comparability of measurements performed with different rheometers and measurement geometries', Materials and Structures, Vol 53, pp 92, 2020
[31] Y. Ogihara, N. Miyazawa. 'Hydraulic characteristics of flow over dam and hydraulic jump of Bingham fluid'. Doboku Gakkai Ronbunshu 1994:485, pp 21-26, 1994